Occupied electronic structure of Au and Ag on Ge(111)

B. J. Knapp,* J. C. Hansen, M. K. Wagner, W. D. Clendening,† and J. G. Tobin
Department of Chemistry, University of Wisconsin–Madison, Madison, Wisconsin 53706
(Received 2 November 1988)

The surfaces formed by the vapor deposition of Au and Ag on $c(2\times8)$Ge(111) were probed with the technique of synchrotron-radiation angle-resolved photoelectron spectroscopy (ARPES), as well as low-energy electron diffraction and Auger-electron spectroscopy. Depositions were performed with the substrate at room and elevated temperatures ($T\approx300$–350 °C) and both the valence and core states were sampled with ARPES. Extensive studies were made of the occupied electronic structure of the $(\sqrt{3}\times\sqrt{3})R30°$ surfaces, which are formed by the deposition of small amounts of Au or Ag onto an elevated-temperature Ge(111) substrate. The results of these experiments indicate that the *d* states of the metal overlayer are atomiclike and that specific occupied electronic states can be associated with the $(\sqrt{3}\times\sqrt{3})R30°$ surface structure. Investigation of the electronic structure of surfaces formed by deposition onto a room-temperature substrate indicates that a bulklike metallic valence-band structure is developing by coverages of 5 or more monolayers. These results and the subtle variations between the Au and Ag systems are discussed.

I. INTRODUCTION

This work is part of a continuing effort to understand the fundamental interactions between metal overlayers and semiconductor substrates. Most of the research in this field has thus far been applied to the technologically important Si substrate. To attain a broader-based understanding of the metal-semiconductor interface, it is desirable to study the interfaces of metals deposited onto other semiconductors, such as Ge.

In this paper we present novel results for the systems Au/Ge(111) and Ag/Ge(111). In particular, the occupied electronic structure of the low-coverage, high-temperature $(\sqrt{3}\times\sqrt{3})R30°$ surfaces and high-coverage, room-temperature overlayers has been probed. These structures, plus insights concerning the growth modes of Au and Ag on Ge(111) at room and elevated temperature, will be discussed. Prior to this study of the occupied electronic structure, other investigations of Au and Ag on Ge(111) had been performed. For example, a study of the unoccupied electronic structure of these same interfaces was recently completed in this laboratory.[1] Previous to that, other investigators have studied various aspects of these interfaces, using a variety of techniques. Extensive investigations of the growth mode of Ag and Au (particularly Ag) for depositions onto a Ge(111) substrate held at room and elevated temperatures are described in Refs. 2–4. The techniques used in their studies include reflection high-energy electron diffraction (RHEED), low-energy electron diffraction (LEED), Auger-electron spectroscopy (AES), and thermal-desorption spectroscopy (TDS). Wachs *et al.*[5,6] and others[7–10] have studied the surfaces formed by deposition of Au and Ag onto near-room-temperature Ge(111) substrates using angle-integrated photoelectron spectroscopies. Core levels and the valence bands were investigated in these experiments. However, to the best of our knowledge, this work and that in Ref. 1 are the first reports of energy- and momentum-resolving studies of the electronic structure of these interfaces.

In this paper we present the results of investigations into the occupied electronic structure of surfaces formed by deposition of Ag and Au onto RT (room temperature) and ET (elevated temperature) $c(2\times8)$Ge(111) substrates. These valence-band and core-level ARPES results will be interpreted in the context of previously presented models for the growth of these overlayers.[2–4] In particular, the interfaces formed by deposition of small amounts [~0.5 monolayers (ML)] of these metals onto an ET substrate were extensively examined. Such evaporation conditions result in a surface known as $(\sqrt{3}\times\sqrt{3})R30°X$/Ge(111), where X = Ag or Au (Refs. 2–4) [these structures will be referred to as $(\sqrt{3}\times\sqrt{3})$Ag or $(\sqrt{3}\times\sqrt{3})$Au]. Similar structures can form by deposition of Ag onto a heated Si(111) substrate[11–19] and comparison of the results and interpretations of the $(\sqrt{3}\times\sqrt{3})$Ag/Ge(111), $(\sqrt{3}\times\sqrt{3})$Au/Ge(111), and $(\sqrt{3}\times\sqrt{3})$Ag/Si(111) interfaces will be made.

High-coverage depositions (≥5 ML) of Au or Ag onto a room-temperature Ge(111) substrate give rise to valence spectra and electronic structures that bear a striking resemblance to those of Au(111) and Ag(111), respectively. The results for these surfaces and the $\sqrt{3}\times\sqrt{3}$ structures, as well as those for a variety of coverages deposited both at room and elevated temperatures, will be compared to previous published growth models.

The remainder of this paper is organized as follows. The experimental procedures and conditions will be described in Sec. II. In Sec. III the results will then be presented and discussed. Finally, a conclusion will be presented in Sec. IV.

II. EXPERIMENT

The experiments were performed in a vacuum chamber containing an angle-resolved photoelectron spectrometer.

The chamber also houses instrumentation for performing (visual observation) LEED and AES with the LEED optics, ion etching, sample heating and manipulation, and metal evaporations. The base pressure in the chamber was near 5×10^{-10} Torr. During heavy evaporations (several monolayers or more) the pressures would rise into the 10^{-9} Torr range.

The 99.999%-pure Ge(111) crystal was purchased,[20] previously cut, and polished to within 1° of the (111) crystallographic plane. The sample is a *p*-type crystal which has been doped with Ga (resistivity of approximately 2.0×10^{-3} Ω cm).[20] A chemical etch of hydrofluoric acid was used to remove the surface layers.[21] *In vacuo* sample cleaning was accomplished by continuous argon-ion etching, at pressures of 10^{-5} Torr, while cycling the temperature of the sample from near room temperature to 600 °C. After these cleaning cycles, the ion etching was stopped and the sample was annealed to temperatures of 600 °C to reorder the surface, as confirmed by LEED observations. The surface displayed a LEED pattern corresponding to the $c(2\times8)$Ge(111) reconstructed surface. In the position of the one-half-order spots, a "crosslike" pattern was observed indicating that the one-eighth- and one-half-order spots were not being resolved. Other authors have made similar observations for Ge(111).[22] AES was performed on the clean, annealed surface to determine levels of contamination. Carbon, sulfur, or oxygen were not observed in the AES spectra above the level of the noise. The noise to Ge (47 eV) signal ratio was approximately 0.004. Similar AES experiments were performed after depositing Ag or Au and after the photoemission measurements were complete. These experiments did not reveal any contamination. However, some contamination peaks are interfered with by adsorbate peaks. For example, in the case of surfaces with Ag overlayers, observation of a potential carbon AES signal (270 eV) is made difficult by a Ag AES peak.

Au or Ag was evaporated by resistively heating a cone of W wire which contained the metal of interest. The W wire was enclosed in a shuttered housing which also contained a quartz-crystal oscillator. The quartz-crystal oscillator was used as a thickness monitor or microbalance and was calibrated through the use of LEED and AES. Typically, this calibration consisted of evaporating Au or Ag onto a heated ($T=300$ °C for Au; $T=350$ °C for Ag) Ge(111) substrate. When the metal AES signal[23] is plotted versus the thickness-monitor reading, a strong "break in slope" at a specific coverage can be observed, as discussed by Le Lay.[2] For the case of Ag, Bertucci *et al.*[4] determined the break in slope to be 0.46 Ag(111) ML.[24] The coverage corresponding to the break in slope for the Au calibration curves has not been as well determined. However, in analogy to the Ag/Ge(111) result and because of the similarity of the Au and Ag LEED and AES observations, as well as their essentially identical lattice parameters, the break-in-slope coverage is assumed to be 0.46 Au(111) ML. Generally, the thickness-monitor output is used as a guide and the ultimate coverage determinations are made by comparing LEED and AES observations to the calibration results. Usually, agreement is quite good. However, in this case the calibration curves are of limited value for determining coverages greater than 0.46 ML. This is due to the small increase in the metal AES signal, as the coverage is increased, for depositions performed on an ET substrate. Coverages were therefore determined by using the calibrated thickness-monitor readout. AES and LEED were performed on all surfaces prepared and these results were internally consistent with the calibration and other previous results. Based on the reproducibility of the calibration curves, it is estimated that the coverages are known to 25% or better.

The ARPES experiments[25] were performed on the 1-GeV storage ring of the University of Wisconsin–Madison Synchrotron Radiation Center (UWSRC), Stoughton, WI, using a spectrometer[25,26] which was built in-house. The spectrometer consists of a hemispherical electron-energy analyzer which is mounted on a two-circle motion goniometer. A double-Einzel lens is mounted on the front of the hemispheres to collect and focus a small solid cone (approximately ±3°) of electrons into the hemispherical analyzer.[26] The pass energy of the analyzer was set at 10 eV and this corresponds to an electron-energy bandpass (full width at half maximum, or FWHM) of 0.070 eV.

In the collection of the data, two different monochromators were used, the normal-incidence monochromator (NIM) and the stainless-steel Seya (SSS) monochromator. The NIM was capable of providing photons from 8 to 50 eV energy through the use of two gratings. The total instrumental bandpass (FWHM) using the high-energy grating of the NIM was experimentally determined from the widths of Fermi-edge steps obtained from spectra of heavy coverages of Ag and Au on Ge(111). Thermal-broadening contributions were removed by subtracting in quadrature. For this grating, the total instrumental bandpass was determined as being 0.11 eV at 18 eV photon energy and increased to 0.16 eV at 50 eV photon energy. Based in part on an evaluation performed by the UWSRC, the total instrumental bandpass using the low-energy grating of the NIM is estimated to be 0.10 eV or less at photon energies of 18 eV or less.[27] The SSS monochromator provided photons from 10 to 30 eV. Generally, parameters that gave rise to a total instrumental bandpass of 0.08 eV at 10 eV photon energy and 0.25 eV at 30 eV photon energy were utilized. However, for surfaces composed of heavy coverages of metal, conditions were modified such that the total-energy bandpass was 0.07 eV at 10 eV photon energy and 0.14 eV at 30 eV photon energy. The energy bandpass values reported here for the SSS monochromator were experimentally determined from Fermi-edge widths as described above. Typically, the linearly polarized light was incident at an angle of 60°, relative to the surface normal. The polarization was in the plane defined by the Poynting vector of the light and the surface normal. Figure 1(a) illustrates the experimental geometry for the in-plane ARPES experiments in which the sampled emission direction was in the plane defined by the incident light and the surface normal. For polar emission angles greater than 50°, an incident angle of 45° was used to reduce the chance of reflecting light into the analyzer. The out-of-plane

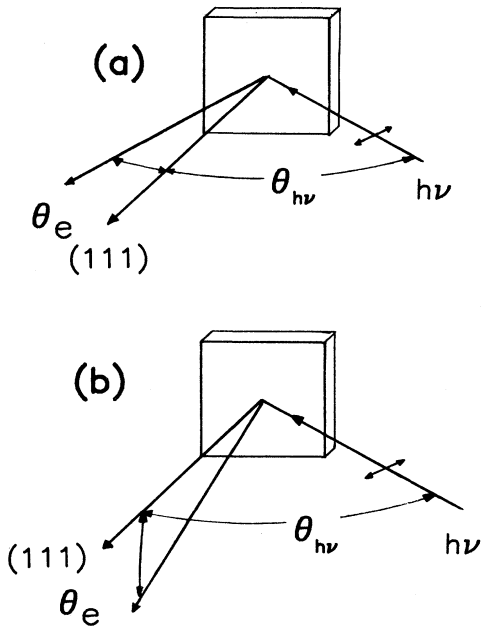

FIG. 1. The sample geometry used in the ARPES experiments is shown in this figure. (a) displays the in-plane geometry, while (b) displays the out-of-plane geometry. For the in-plane geometry, an angle of incidence of the light of 60°, relative to the surface normal, was used for angles of emission from 0° to 50°. For angles of emission greater than 50°, an angle of incidence of 45° was used to avoid reflecting light into the analyzer. The angle of incidence for all of the out-of-plane experiments was 60°.

geometry is shown in Fig. 1(b). In this geometry the emission plane and incident light plane are perpendicular to one another. The incident angle for all of the out-of-plane experiments was 60°.

Orientation of the samples was performed through the use of laser alignment and LEED. An estimate of the error associated with these techniques is 1°. The samples were at or near room temperature for all of the photoemission measurements.

III. PHOTOEMISSION RESULTS AND DISCUSSION

This section is organized as follows. The results concerning the Ag/Ge(111) system will be discussed before those of the Au/Ge(111) system. For each metal, the growth modes at RT and ET will be described and the $\sqrt{3}\times\sqrt{3}$ structure will be analyzed.

A. Ag/Ge(111)

1. Growth modes and high-coverage depositions

The growth modes of Ag on Ge(111) have been previously reported in Refs. 2–4. It was determined that very different growth modes occur depending upon the substrate temperature during deposition. For depositions performed on a RT Ge(111) substrate nearly layer-by-layer growth occurs whereas for depositions performed on an ET substrate the growth mode is Stranski-Krastanov (completion of a layer followed by island growth). Furthermore, it was determined that the AES break-in-slope coverage (0.46 ML) corresponds to the completion of the $(\sqrt{3}\times\sqrt{3})$Ag structure.[4] Generally, the results of the combined LEED, AES, and ARPES investigation presented here are in agreement with those previously reported observations and their proposed growth modes of Ag on Ge(111), both at RT and ET. Slight deviations were observed and those are described elsewhere.[28] Because of their novelty, the ARPES results will be emphasized here.

The strong dependence of the spectra and electronic structure of the Ag/Ge(111) interface upon both coverage and substrate temperature is illustrated in Fig. 2. In this figure are normal-emission photoelectron spectra obtained from surfaces prepared both with the Ge at RT and ET. These spectra were acquired using a photon energy of 50 eV on the NIM. Data were also collected at other photon energies ($h\nu$=10, 18, 21, 30, and 40 eV), which also often exhibited the characteristics described below. The spectra include both the valence bands and the Ge 3*d* core level near B^F=30 eV. (Note that B^F is the binding energy with respect to the Fermi energy. As mentioned above, Fermi energies can be determined from high-coverage, room-temperature depositions.) The spec-

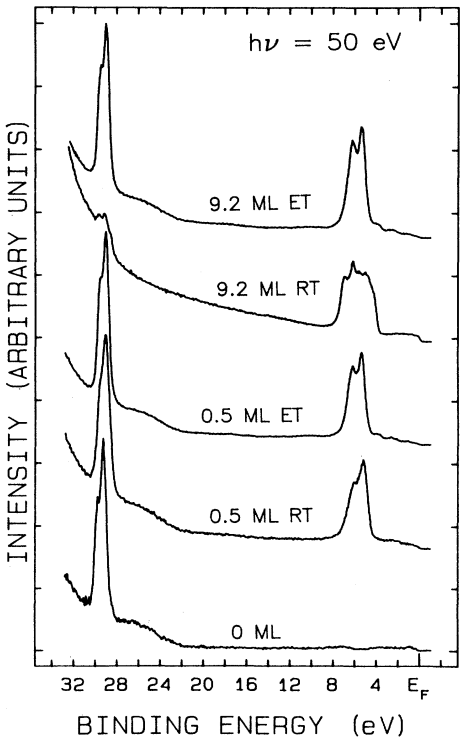

FIG. 2. Normal-emission ARPES spectra obtained with 50 eV photon energy are shown in this figure. Spectra of samples prepared by deposition of Ag onto a substrate at room and elevated temperature are included.

tral structure in the region of the valence bands changes dramatically upon addition of 0.5 ML of Ag onto either a RT or ET Ge(111) substrate, relative to the spectrum obtained from a clean Ge(111) surface. The prominent features observed near $B^F = 5-6$ eV are due to the Ag 4*d* valence states. These states have a large photoionization cross section relative to that of the Ge valence bands and dominate the low-B^F region of the spectra at this photon energy.[29] Small but significant differences in the binding energies of the Ag 4*d* features can be observed between the spectra obtained from surfaces prepared at RT and ET. The Ag 4*d* states from surfaces prepared at ET are at larger values of B^F (5.3 and 6.2 eV) than those states for surfaces prepared at RT (5.2 and 6.0 eV). Dissimilarities were likewise discerned in the LEED patterns. The $(\sqrt{3}\times\sqrt{3})$Ag pattern was seen in the case of the surface prepared at ET. The LEED pattern from the surface prepared at RT resembled that which could be expected from a layer or islands with a Ag(111)-like structure, growing in both perpendicular and parallel epitaxy to the Ge(111) substrate.[28] [It is not clear to us, however, what the structure of this RT Ag/Ge(111) surface is.] These observations indicate that the surface structures associated with depositions of 0.5 ML of Ag onto a RT and ET substrate are different.

More pronounced variations between the spectral features of the RT and ET interfaces can be seen at higher coverages. Spectra from surfaces prepared by deposition of 9.2 ML of Ag onto a RT and ET substrate are also shown in Fig. 2. But before discussing the differences between the 9.2-ML ET and RT spectra, the following will be considered. The 9.2-ML ET spectrum is strikingly similar to the one obtained from the surface prepared by deposition of 0.5 ML of Ag onto an ET substrate. This result is somewhat surprising. In view of the increase of coverage of nearly 20-fold, one would expect to see considerable change in the electronic structure of the valence bands. Normal-emission ARPES spectra were obtained from surfaces prepared by deposition of 9.2, 18.4, and 55.2 ML of Ag onto an ET substrate at this and other photon energies (not shown).[28] These data indicate that only a slight perturbation of the Ag 4*d* features can be observed even at very large coverages. The ARPES results described here are consistent with those reported in AES studies[2,4] of such surfaces prepared at ET. In those AES investigations, it was reported that the Ag AES signal (350 eV) does not increase substantially with increasing coverage nor does the LEED pattern lose its $\sqrt{3}\times\sqrt{3}$ characteristics, for coverages greater than the break in slope. We have duplicated these AES and LEED results in parallel with our ARPES studies in order to provide an absolute correlation. The earlier LEED and AES observations were interpreted in terms of a Stranski-Krastanov growth model where the $(\sqrt{3}\times\sqrt{3})$Ag structure is complete at 0.46 ML and where at increasing coverages Ag(111)-like islands are forming on top of the $\sqrt{3}\times\sqrt{3}$ surface.[2] If the surface area covered by the islands is not increasing with coverage, then the signal (both ARPES and AES) should not change appreciably with increasing metal deposition. This suggests that significant areas of the surface are apparently not covered until 18.4–55.2 ML of Ag has been deposited. These hypotheses are also supported by the LEED patterns observed from these surfaces. A LEED pattern corresponding to the $(\sqrt{3}\times\sqrt{3})$Ag structure is observed at all of these coverages, indicating that the islands are not affecting the long-range order on the surface. Note, however, that the interpretation here is made entirely in the context of the model developed earlier. While our results are consistent with this model, we cannot rule out completely the possibility of other geometrical growth modes.

Now let us return to consideration of the temperature-induced variations of the electronic structure at 9.2 ML, as illustrated in Fig. 2. The spectrum of the surface formed by the deposition of 9.2 ML of Ag onto a RT substrate is very different than that obtained from the surface formed by deposition of the same amount of Ag onto an ET substrate. This observation is consistent with and supportive of the previously proposed growth models for ET and RT deposition. The growth mode of Ag on Ge(111) at RT has been described as nearly layer by layer[2,4] which would result in a substrate signal that is attenuated as the coverage is increased. This decrease in signal can be observed in the spectrum of 9.2 ML of Ag deposited onto a RT Ge(111) substrate: the Ge 3*d* core peak is attenuated relative to the 0.5-ML spectrum prepared under the same conditions. Additionally, the valence bands are broadened and steplike emission is seen at E_F. These observations are consistent with bulklike, metallic behavior of the overlayer.

Moreover, there is strong evidence that the higher-coverage, room-temperature depositions are not only metallic and bulklike but are specifically developing structure that strongly resembles that of bulk Ag(111). It has been reported that RHEED and LEED patterns of heavy depositions of Ag onto RT Ge(111) resemble those of Ag(111).[2–4] These LEED observations are consistent with the results of our study, in which the electronic structure was probed using monochromatic light of many different energies. An example of our data is shown in Fig. 3: normal-emission ARPES spectra, obtained on the NIM at 21 eV photon energy, exhibit a very rapid development of spectral structure that is almost identical to that of Ag(111).[30] (The conditions in Ref. 30 have been closely duplicated in our study, to facilitate comparison of spectra.) However, there is one major discrepancy: the Ag(111) Shockley surface state near E_F was not observed for the Ag/Ge(111) system. These observations would indicate that the Ag overlayer on the Ge surface has developed bulk-band structure similar to Ag(111), but that the surface of the overlayer is not quite the same as Ag(111).

Further information concerning this hypothesis of surface imperfections can be gleaned from other techniques, such as core-level measurements. Wachs, Miller, and Chiang[6] have reported that a small amount of Ge "floats" on top of the developing Ag overlayer for depositions of Ag onto a near-RT $c(2\times8)$Ge(111) sample. This "floating" Ge could interfere with the formation of the Ag(111)-like surface state, particularly in light of the two-dimensionally delocalized nature of the Ag(111) sur-

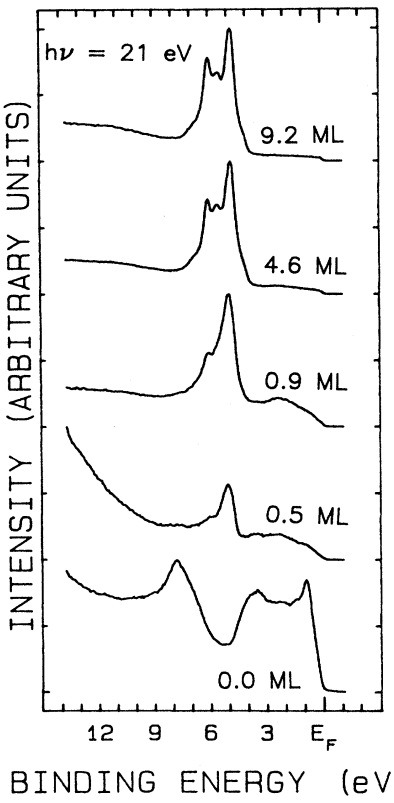

FIG. 3. Normal-emission ARPES spectra obtained at 21 eV photon energy are displayed in this figure. The surfaces were prepared by deposition of Ag onto a room-temperature Ge(111) substrate. The development of Ag(111)-like behavior can be observed by coverages near 4.6 ML.

face state.[31] Additionally, the unoccupied version of this surface state has been probed with k-resolved inverse photoemission. It was reported in Ref. 1 that a spectral feature, corresponding to the Shockley-type Ag(111) surface state near E_F, was observed for the Ag/Ge(111) system. This raises the question: why is the state observed with inverse photoemission but not ARPES? The answer may lie in the magnitude of the coverages used. In the ARPES experiments, coverages as large as 18.4 ML were deposited onto a RT substrate and a Ag(111)-like surface state was not observed in the normal-emission spectra at any photon energy studied (10, 18, 21, 26, and 30 eV). The coverages used in the inverse-photoemission study were very much larger [50–120 Ag(111) ML] and it is believed that the floating Ge is trapped in the developing overlayer with these very heavy depositions of Ag, allowing the formation of the Ag(111)-like surface state.

2. $(\sqrt{3}\times\sqrt{3})$Ag/Ge(111)

We now turn our attention to the highly ordered structure which forms at elevated substrate temperatures, the $\sqrt{3}\times\sqrt{3}$ surface. The Stranski-Krastanov growth mode has been reported to be occurring for depositions of Ag onto an ET Ge(111) substrate.[2] This growth model consists of the following: the formation of a $(\sqrt{3}\times\sqrt{3})$Ag structure, which is completed at 0.46 Ag(111) ML, and the development of Ag(111)-like islands on top of this $(\sqrt{3}\times\sqrt{3})$Ag structure at higher coverages.[4] In this study, extensive ARPES experiments have been performed to evaluate the occupied electronic structure of the $(\sqrt{3}\times\sqrt{3})$Ag surface. Surfaces were prepared for these studies by depositing 0.46 ML onto a 350-°C Ge(111) substrate. This should result in a surface which is singular in nature: islands should not have formed nor should clean Ge(111) be exposed. This coverage was chosen so that the spectral features could be related directly to the $(\sqrt{3}\times\sqrt{3})$Ag structure. The ARPES experiments consist of both normal-emission and off-normal-emission measurements.

The normal-emission experiments were performed on the NIM at photon energies from 8 to 40 eV. These measurements test the dependence of the binding energies upon momentum perpendicular to the surface.[25] The polarization of the light was in the plane defined by the surface normal and the $\langle 1\bar{1}0\rangle$ direction in the bulk Ge(111) crystal [$\bar{\Gamma}$–$\bar{K}$ azimuth of the (1×1)Ge(111) surface Brillouin zone (SBZ)]. Off-normal-emission ARPES experiments were performed on the SSS monochromator. These spectra were collected with two different photon energies (18 and 26 eV). Off-normal experiments test the dependence of the binding energies upon momentum parallel to the surface. Using two different photon energies allows for different combinations of momenta parallel and perpendicular to the surface.[25] The spectra collected at 26 eV were more sensitive to the Ag 4d spectral features than those obtained at 18 eV photon energy. The off-normal-emission experiments were performed in two different experimental geometries, as shown in Fig. 1. For both geometries the light is predominantly p polarized. Two different high-symmetry azimuths of the (1×1)Ge(111) surface Brillouin zone (SBZ) were probed in these off-normal-emission measurements. These were the $\bar{\Gamma}$–$\bar{K}$ azimuth ($\langle 1\bar{1}0\rangle$ direction) and the $\bar{\Gamma}$–$\bar{M}$ azimuth ($\langle 1\bar{2}1\rangle$ direction). The results from these ARPES measurements of the $(\sqrt{3}\times\sqrt{3})$Ag surface are all consolidated into Fig. 4. In Fig. 4(a) the B^F of the spectral features versus photon energy is plotted for the normal-emission measurements. This plot is shown versus photon energy (and not momentum) due to lack of knowledge about the final states for this surface. However, it still remains a strong test of the dependence of B^F upon the component of momentum perpendicular to the surface.[25] The B^F of the spectral features versus the component of momentum parallel to the surface for the $(\sqrt{3}\times\sqrt{3})$Ag surface is plotted for both the $\bar{\Gamma}$–$\bar{M}$ and $\bar{\Gamma}$–$\bar{K}$ azimuths in Figs. 4(b) and 4(c). [The horizontal scale of Figs. 4(b) and 4(c) is arrived at by assuming that the component of the momentum, of an electron, parallel to the surface is conserved.[25]] The in-plane and out-of-plane measurements as well as the results from spectra obtained at 18 and 26 eV photon energy are all represented in this figure. Spectra from $c(2\times8)$Ge(111) were obtained under identical experimental conditions as those from the $(\sqrt{3}\times\sqrt{3})$Ag surface for both the normal and off-normal experiments. Spectral features that are clearly related to

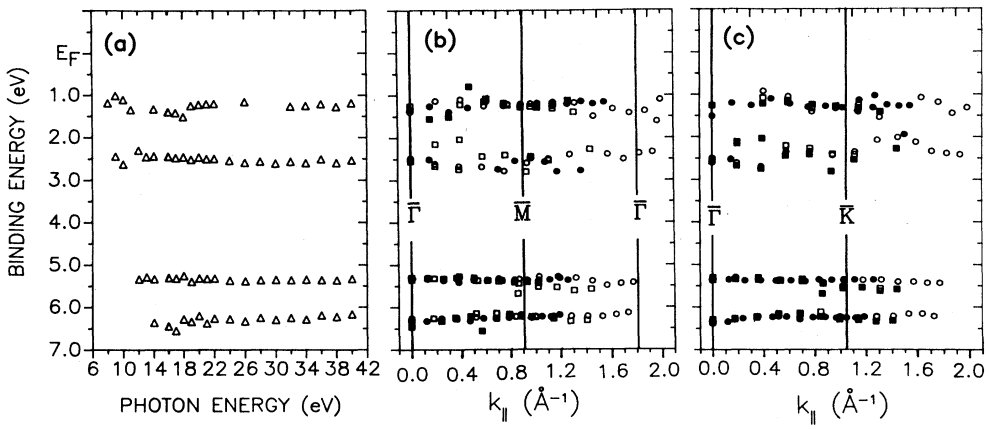

FIG. 4. This figure condenses all of the ARPES experiments performed on the $(\sqrt{3}\times\sqrt{3})$Ag surface. A plot of the B^F vs photon energy for the normal-emission spectral features is shown in (a). (b) and (c) display B^F vs the parallel component of momentum for the $\bar{\Gamma}-\bar{M}$ and $\bar{\Gamma}-\bar{K}$ azimuths, respectively. The open (solid) symbols represent data obtained with a photon energy of 26 eV (18 eV). The circles (squares) depict data obtained in the in-plane (out-of-plane) geometry.

bulk Ge(111) are not shown in Fig. 4. (All of the data and B^F plots are available in Ref. 28.) This elimination of Ge bulklike features was done to simplify the analysis of the features resulting from the $(\sqrt{3}\times\sqrt{3})$Ag structure. The underlying Ge spectral features may occasionally be contributing due to the difficulty of differentiating between features at similar binding energies. The ARPES spectra from the $(\sqrt{3}\times\sqrt{3})$Ag surface do not display steplike intensity at the Fermi energy. Therefore the analyzer potentials corresponding to the Fermi energy were determined from surfaces of heavy coverages of Au and Ag on Ge(111) and these potentials were then used to determine B^F for the $(\sqrt{3}\times\sqrt{3})$Ag surfaces. The standard deviation of these potentials was 0.023 eV or less for all photon energies studied on both monochromators, indicating the quality of the measurements. The implications of Fig. 4 will be discussed below.

Four different bands can be observed in Fig. 4 which do not disperse (or disperse only weakly) with either photon energy (perpendicular component of momentum) or the parallel component of momentum. The features at $B^F=5.3$ and 6.2 eV can be assigned to the Ag 4*d* states. The nondispersive behavior of these spectral features is indicative of atomiclike behavior where the states do not show a dependency on momentum. The splitting of these Ag 4*d* features is 0.88 ± 0.05 eV. This value is considerably greater than the spin-orbit-splitting parameter of the Ag 4*d* states [$\xi\approx0.2$ eV,[25,32] which can cause a splitting in atomic systems between the $4d_{3/2}$ and $4d_{5/2}$ of 0.56 eV (Ref. 32)] and suggests that factors other than spin orbit, such as crystal-field and band effects, are playing an important role in the splitting of the Ag 4*d* states. The intensities of these Ag 4*d* features (relative to one another) vary with emission angle. However, the intensities do not display a dependency upon the azimuth of the substrate or on the geometry for the data collection (in plane versus out of plane).

Another nondispersive band can be observed at $B^F=2.5$ eV. This feature is apparently related to the $\sqrt{3}\times\sqrt{3}$ surface structure as it is observed in the ARPES spectra of $(\sqrt{3}\times\sqrt{3})$Ag and $(\sqrt{3}\times\sqrt{3})$Au (to be discussed below), but not in spectra of clean Ge(111) or surfaces prepared by deposition of large amounts of Au or Ag onto a room-temperature substrate. The feature does not disperse with momentum (parallel or perpendicular) and this observation suggests the localized or possibly atomic nature of this peak. The peak becomes very weak for experiments performed off normal. Thus, the B^F determination becomes less precise at nonzero values of the parallel component of momentum. An intensity maximum for normal emission at photon energies of 24–26 eV is observed. This behavior is different than the Ag 4*d* states and may be indicative that the feature is either not related to the Ag 4*d* states or is related but strongly perturbed.

A nondispersive or weakly dispersive band is observed at $B^F=1.2$ eV. The intensity oscillations of this feature are similar to those of a peak which has been assigned as a surface state of Ge(111) at $B^F=1.4$ eV.[31] At least one other surface state has been reported for the clean Ge(111) surface at $B^F=0.8$ eV (Ref. 33): this feature is not seen in the case of the $(\sqrt{3}\times\sqrt{3})$Ag surface. The attenuation of a surface-related feature is not surprising. One of the most commonly used probes of surface states is to test for a reduction of their intensity upon contamination. The observation of a $(\sqrt{3}\times\sqrt{3})$Ag feature similar to a surface state of clean Ge(111) may indicate that major structural changes in the surface have not occurred.

Next, the Ge 3*d* core peaks will be considered. The spectra of the Ge 3*d* core levels from clean $c(2\times8)$Ge(111) surfaces display a small shoulder at a lower B^F than the bulk peaks (approximately a 0.75-eV shift).[5] This feature has been described as intensity due to adatoms on the surface of the reconstructed Ge surface.[5] Spectra of the Ge 3*d* core from the $(\sqrt{3}\times\sqrt{3})$Ag

surface, obtained on the NIM at normal emission with 50 eV photon energy, do not display a feature at a lower B^F. This may indicate that the adatoms are not present in this $(\sqrt{3}\times\sqrt{3})$ Ag surface structure, or that the environment of these atoms has changed and resulted in a shift of the feature to higher binding energy. If this were the case, then the observation of this weak core feature would be made very difficult by the bulk component. It should be mentioned that an overall shift of 0.16 eV toward a lower binding energy was observed in the core spectra of the $(\sqrt{3}\times\sqrt{3})$Ag surface [compared to the $c(2\times8)$Ge(111)] and this has been attributed to band bending for this interface.

Comparison of the Ag/Ge(111) system to the Ag/Si(111) system reveals many similarities. The growth modes with the substrate at RT or ET are very similar.[2] Moreover, both systems exhibit LEED patterns corresponding to the $\sqrt{3}\times\sqrt{3}$ structure for depositions performed on an ET substrate.[2] ARPES experiments performed on the $(\sqrt{3}\times\sqrt{3})$Ag/Si(111) system have demonstrated nondispersive behavior of the Ag 4*d* states,[15] and the splitting observed between these Ag 4*d* features is near 0.9 eV.[15] Furthermore, the Ag 4*d* states are more deeply bound for the $(\sqrt{3}\times\sqrt{3})$Ag/Si(111) system than for the surfaces prepared by deposition of Ag onto a RT substrate.[15] All of these observations are similar to those for the Ag/Ge(111) system. These observations suggest that the occupied electronic structures of the two systems are very much the same and the geometrical structures may, likewise, be similar. It has been previously reported that the *unoccupied* electronic structures of these two systems also bear a strong resemblance to each other.[1] Because of the strong similarity of the two interfaces, it is useful to consider here the proposed structural models for the $(\sqrt{3}\times\sqrt{3})$Ag/Si(111).

Scanning-tunneling-microscopy (STM) studies of the $(\sqrt{3}\times\sqrt{3})$Ag/Si(111) surfaces have been performed.[11–13] Two models have been proposed by the authors of these studies and other research:[14] the embedded Ag trimer model and the honeycomb model. As mentioned above, it is reasonable to evaluate our ARPES and other results in light of these two models. In both of the models the Ag 4*d* states can be expected to display atomiclike behavior. In the case of the honeycomb model, the Ag atoms are separated from each other by considerable distances and this would preclude overlap of the generally localized Ag 4*d* electrons. (The localized and directionalized nature of 4*d* orbitals also implies that bonding between the Ag 4*d* states and the Ge states would tend to be hindered,[25] in almost any model.) The embedded-Ag-trimer model predicts that the Ag atoms exist as trimers in the semiconductor double layer,[11,12] raising the possibility of *d-d* overlap. However, studies concerning small metal clusters have suggested that bulklike behavior should not be expected for clusters that are less than 100 atoms.[34] Therefore, trimer units seem to be unlikely candidates for displaying bulklike dispersive behavior in the Ag 4*d* orbitals. Finally, neither of these models predicts Ge adatoms on the surface. The observation that the adatom-related core feature is not visible in the Ge 3*d* core spectra, for the $(\sqrt{3}\times\sqrt{3})$Ag surface, is consistent with both models. Thus, we are unfortunately unable to differentiate between these models using our ARPES data and must conclude that either is plausible for $(\sqrt{3}\times\sqrt{3})$Ag/Ge(111).

B. Au/Ge(111)

1. Growth modes and high-coverage depositions

Studies of the growth modes of Au on Ge(111) were conducted in a manner which is very similar to the case of Ag/Ge(111). LEED, AES, and ARPES were all used to investigate this interface. The LEED and AES results obtained in this study compare favorably to those previously published.[2] As with the Ag/Ge(111) interface, the ARPES results will be emphasized.

The growth modes of Au/Ge(111) with the substrate held at RT and ET (300 °C) have been previously investigated.[2] These studies suggest that the Stranski-Krastanov growth mode occurs for deposition of Au onto an ET substrate.[2] The case for deposition of Au onto a RT substrate is not as well determined. Some investigators have proposed that the interface is strongly intermixed,[5,8–10] while others have suggested that island formation of the Au on the Ge(111) interface cannot be ruled out.[35] The results obtained in the research presented here suggest that the growth modes and structures of the Au/Ge(111) interface are not significantly different for surfaces prepared at RT and ET. This observation is very different than that for the case of Ag/Ge(111). Our discussion will be broken into two parts: first we will consider coverages of less than or equal to $\frac{1}{2}$ ML, which is associated with the completion of the $\sqrt{3}\times\sqrt{3}$ structure; then, higher coverages will be discussed.

Comparison of photoemission results obtained from surfaces prepared by deposition of 0.5 ML of Au onto an ET and RT substrate reveals definite similarities: the binding energies and widths of the Au 5*d*'s are much the same in both cases. Furthermore, a peak near 2.4 eV, previously identified as being related to the $\sqrt{3}\times\sqrt{3}$ structure, can be seen in the ARPES spectra obtained from surfaces prepared at either RT or ET. Additionally, surfaces prepared by deposition of 0.5 ML of Au onto a RT substrate give evidence of a weak $\sqrt{3}\times\sqrt{3}$ LEED pattern, the same pattern as for surfaces prepared at ET. All of these observations suggest that the structures at low coverages for surfaces prepared at RT and ET are closely related. These trends are very different than those for the case of Ag/Ge(111), where the depositions performed at ET and RT give rise to what are apparently very dissimilar growth modes.

Bridging the two coverage regimes are the Auger-intensity measurements. The plots of Au AES intensity versus coverage for depositions performed onto an ET substrate show a strong and distinct break in slope near a coverage of 0.5 Au(111) ML.[2] Depositions performed onto a RT substrate result in a less distinct break or a "knee" in the curve of Au AES intensity,[2] occurring at a coverage of about 1 ML. As mentioned above, the growth mode at ET has been reported as being Stranski-Krastanov,[2] with the assumed completion of the

$\sqrt{3}\times\sqrt{3}$ structure at $\frac{1}{2}$ ML. It seems plausible that much the same process is also occurring at RT, but in a less perfect fashion: in the ET growth, island formation follows the completion of the $\sqrt{3}\times\sqrt{3}$, two-dimensional layer, whereas, at RT, island formation begins before the completion of the $\sqrt{3}\times\sqrt{3}$, delaying the bending over of the AES curve and the presumed completion of the $\sqrt{3}\times\sqrt{3}$ structure until coverages closer to 1 ML. Unfortunately, the utility of such AES measurements is limited and we cannot rule out other explanations. Additionally, no determinations of microscopic structure have been reported to date. However, some information concerning the island growth at higher coverages is available. RHEED observations of heavy depositions of Au onto Ge(111) at RT have suggested that the islands are Au(111)-like and are growing in parallel epitaxy.[3] The ARPES measurements discussed below confirm the Au(111) nature of the overlayer at higher coverages.

Normal-emission ARPES measurements provide a direct means of probing whether a high-coverage overlayer is developing toward a specific bulk electronic structure.[25] In this case, we are testing if the overlaying of Au is converging to an electronic structure similar to Au(111). These normal-emission ARPES studies were conducted over a wide photon-energy range upon surfaces prepared by deposition of 36.8 ML of Au onto a RT substrate. The spectra were obtained with the same geometry as was used for the normal-emission ARPES investigations of Ag/Ge(111) discussed above. A plot of the B^F versus photon energy of the electronic states of this Au/Ge(111) surface is shown in Fig. 5(a). For comparison, Fig. 5(b) displays a B^F–versus–photon-energy plot of clean Ge(111). Obvious differences between the two plots can be seen, supporting the notion that the electronic structure of this high-coverage surface is dominated by the Au, not the Ge. Comparisons of Fig. 5(a) to similar plots for Au(111) and Au(111)-like surfaces[36] reveal strong similarities. Moreover, spectra of this high-coverage Au/Ge(111) surface bear a very strong resemblance to those obtained from Au(111) under similar experimental conditions.[37] These observations suggest that the surface produced by deposition of 36.8 ML of Au onto a RT substrate is Au(111)-like. This is not to say that the surface is necessarily an overlayer of Au(111) that is 36.8 ML thick. Rather, it may be that islands are growing on the surface and have some sort of structure that is similar to Au(111) and they are coalescing to irregularly cover the surface. Additionally, a major difference was found between the spectra obtained from the Au/Ge(111) system and those of Au(111): the Au(111) surface state near E_F was not observed for the Au/Ge(111) system. This result is very similar to that found in the Ag/Ge(111) system and seems to suggest that Ge is floating on top of the developing Au overlayer. Unfortunately, other direct measurements, such as Ge 3*d* core-level spectra, that could provide a test of this hypothesis are not available for this interface.

We have also performed a parallel investigation using an ET substrate. Deposition of 18.4 ML of Au onto an ET substrate resulted in spectra and a B^F–versus–photon-energy plot that is similar to that of

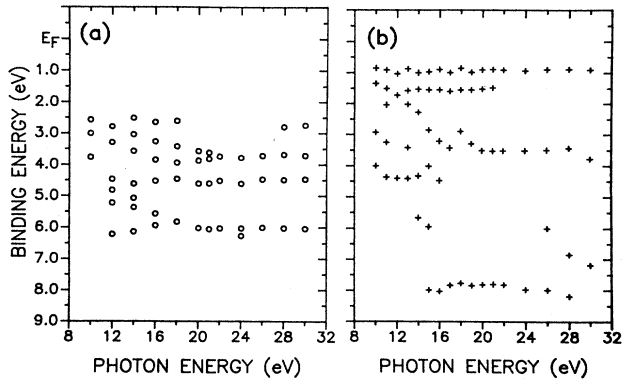

FIG. 5. A plot of B^F vs photon energy for ARPES spectra obtained at normal emission is shown for a surface prepared by deposition of 36.8 ML of Au onto a room-temperature Ge(111) substrate, in (a). A similar plot for a clean $c(2\times8)$Ge(111) surface is shown in (b).

Au(111) (Ref. 37) and to the Au/Ge(111) surfaces prepared at RT. In fact, the development of Au(111)-like spectral features with increasing coverage appears to be much the same for surfaces prepared at RT and ET. These ARPES results for high-coverage Au/Ge(111) support the hypothesis that the growth mode of Au on Ge(111) is not very different for depositions performed at RT and ET and are consistent with the AES results discussed above.

Before going on to the $\sqrt{3}\times\sqrt{3}$ Au surface, it is worthwhile to consider the differences between the Au and Ag systems more carefully. The observation that a metal (111)-like surface forms for depositions of Au onto an ET substrate is at variance with the results of the case of Ag on Ge(111). Even for coverages of 55.2 ML of Ag deposited onto an ET substrate, Ag(111)-like ARPES spectra were not obtained. Additionally, the intensity increase of the AES signal of the metal overlayer for the two systems is different. For the case of Ag, very little increase is observed as the coverage is increased above 0.46 ML, while for the case of Au a greater increase is observed.[2] These observations may be due to different island morphologies for the two systems. The islands of the Ag/Ge(111) system are apparently not covering as much of the surface as those of the Au/Ge(111) system, for similar coverages. This would result in more of the $(\sqrt{3}\times\sqrt{3})$Ag structure being exposed, for a given coverage, than the corresponding $(\sqrt{3}\times\sqrt{3})$Au structure. Therefore, more Ag is required to observe changes in the spectral features than Au. The LEED observations also support this hypothesis. Au(111)-like LEED patterns (perpendicular and parallel epitaxy) could be observed for deposition of 4.6 ML of Au onto an ET substrate, whereas for Ag depositions performed under similar conditions only the $(\sqrt{3}\times\sqrt{3})$Ag LEED pattern could be observed. This suggests that Au(111)-like islands were forming with long-range order sufficient to produce diffraction patterns while similar structures did not exist for the case of Ag.

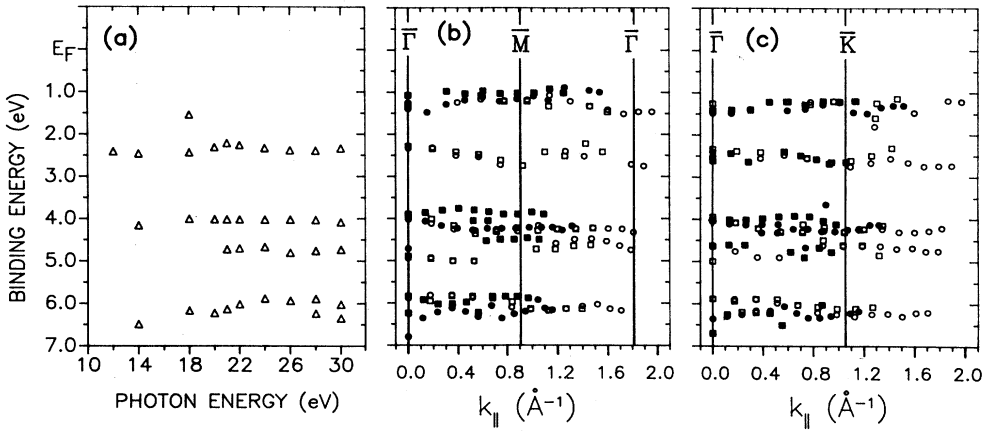

FIG. 6. This figure depicts the ARPES results from the $(\sqrt{3}\times\sqrt{3})$Au surface. The plot of B^F vs photon energy of normal-emission spectral features is shown in (a). (b) and (c) depict the off-normal ARPES results obtained in the $\bar{\Gamma}$–$\bar{M}$ and $\bar{\Gamma}$–$\bar{K}$ azimuths, respectively. The open (solid) symbols represent data obtained at 26 eV (18 eV) photon energy. The circles (squares) depict data obtained in the in-plane (out-of-plane) geometry.

2. $(\sqrt{3}\times\sqrt{3})$*Au/Ge(111)*

Extensive experiments were performed on surfaces prepared by deposition of 0.5 ML of Au onto an ET Ge(111) substrate. According to the Stranski-Krastanov growth mode, this surface should be very singular in nature. These experiments were performed in the same format as the $(\sqrt{3}\times\sqrt{3})$Ag studies. The geometries and photon energies used are generally the same as the $(\sqrt{3}\times\sqrt{3})$Ag experiments, except that the normal-emission experiments were performed on the SSS using photon energies from 10 to 30 eV. The results of these normal- and off-normal-emission measurements are shown in Fig. 6. As for the case of Ag/Ge(111), the features clearly related to bulk Ge have been removed from this figure. The Au 5*d* states[28] near $B^F=4.0$, 4.4, and 6.0 eV can be seen in these plots. Ge features near 4.0 eV could not be easily separated from the Au 5*d* features close to this energy and, therefore, the B^F values of these features are not as well determined as for the features near 6.0 eV. In general, the binding energies of the Au 5*d* features are not as well resolved as those of the Ag 4*d* features. This may be due in part to the increased spin-orbit-splitting parameter of Au ($\xi_{5d}\approx 0.7$ eV, Ref. 37) versus Ag ($\xi_{4d}\approx 0.2$ eV, Refs. 25 and 32). For example, the larger spin-orbit effect in Au may be the underlying cause of the observation of a third metal *d* feature in $(\sqrt{3}\times\sqrt{3})$Au, but not in $(\sqrt{3}\times\sqrt{3})$Ag. The splitting between the two most obvious Au 5*d* features is 1.91 eV while the predicted splitting for the Au $5d_{3/2}$ and $5d_{5/2}$ is 1.77 eV.[37] The fact that the experimental separation is greater than pure spin-orbit splitting and that three peaks are observed suggests that factors other than spin orbit (such as crystal-field and band effects) are playing a role in the splitting of these features. These trends concerning the splitting of the Au 5*d* states in $(\sqrt{3}\times\sqrt{3})$Au are similar to those for the Ag 4*d* states in the $(\sqrt{3}\times\sqrt{3})$Ag surface. The results summarized in Fig. 6 suggest that the Au 5*d* states are at most weakly dispersive with momentum parallel or perpendicular to the surface. These observations parallel the ones made for the $(\sqrt{3}\times\sqrt{3})$Ag system, although the dispersion appears to be stronger in the $(\sqrt{3}\times\sqrt{3})$Au surface. Further similarities between the two systems will be discussed below.

A nondispersive or weakly dispersive band near 2.4 eV can be seen in Fig. 6. This feature displays intensity oscillations with photon energy and the parallel component of momentum similar to those of the state at 2.5 eV on the $(\sqrt{3}\times\sqrt{3})$Ag surface. This peak has been attributed to the $\sqrt{3}\times\sqrt{3}$ surface structure since it is not observed in the spectra of clean Ge(111) and is present in those of the $(\sqrt{3}\times\sqrt{3})$Ag and $(\sqrt{3}\times\sqrt{3})$Au surfaces. Additionally, a feature at $B^F=1.2$ eV can also be observed in Fig. 6 and it displays intensity oscillations similar to those of the feature near 1.2 eV from the $(\sqrt{3}\times\sqrt{3})$Ag surface. Again, it seems likely that this feature is related to a surface state observed on the reconstructed Ge(111) surface, as discussed above for the case of $(\sqrt{3}\times\sqrt{3})$Ag.

The $(\sqrt{3}\times\sqrt{3})$Ag and $(\sqrt{3}\times\sqrt{3})$Au systems generally exhibit trends in the data that parallel one another. This implies that the *occupied* electronic structures of these two systems are very similar. Furthermore, it has been proposed that the *unoccupied* electronic structures of these two systems are also alike.[1] These observations concerning electronic structure imply that the geometrical structures for these $\sqrt{3}\times\sqrt{3}$ surfaces are much the same and the $\sqrt{3}\times\sqrt{3}$ surfaces of Ge(111) are closely analogous to the $(\sqrt{3}\times\sqrt{3})$Ag/Si(111) surface, as discussed above.

IV. CONCLUSIONS

Extensive normal and off-normal ARPES experiments were performed on the $(\sqrt{3}\times\sqrt{3})$Ag and $(\sqrt{3}\times\sqrt{3})$Au surfaces. These results indicate that the occupied electronic structure of these two surfaces is similar to one

another and to the $(\sqrt{3}\times\sqrt{3})$Ag/Si(111) interface. The metal d states do not display strongly dispersive behavior. This observation is suggestive of atomiclike d states. A feature near 2.5 eV, B^F, was observed for these $\sqrt{3}\times\sqrt{3}$ surfaces and is apparently specific to this $\sqrt{3}\times\sqrt{3}$ structure. A peak that may correspond to a surface state observed on the $c(2\times8)$ Ge(111) surface is also observed near 1.2 eV. These $\sqrt{3}\times\sqrt{3}$ surfaces may be interpreted in the context of two suggested models for the $(\sqrt{3}\times\sqrt{3})$Ag/Si(111) interface. Both models are consistent with our results, but we cannot differentiate between the two.

Room-temperature deposition of high coverages of either Ag or Au onto Ge(111) results in surfaces which display bulk-band behavior that parallels that of the corresponding metal (111) surface. The Shockley-type surface states associated with these metal (111) surfaces were not observed, consistent with the notion the Ge is floating on top of the metal depositions.

The growth modes of Ag and Au on Ge(111) have been investigated, with the substrate at room and elevated temperature. Basically, our results are consistent with previous observations and models of Le Lay *et al.*,[2] except that we propose that the growth mode of Au/Ge(111) is Stranski-Krastanov at both room and elevated temperatures.

ACKNOWLEDGMENTS

We are grateful for the support that we have received from the following individuals and institutions: the Eastman Kodak Company (Rochester, NY); the Camille and Henry Dreyfus Foundation, Inc. (New York, NY); the Research Corporation (Tucson, AR); the Rohm and Haas Company; the donors of the Petroleum Research fund, administered by the American Chemical Society; Amoco Foundation, Inc.; and the National Science Foundation (under Grant No. DMR-84-19262). R. de Souza-Machado aided in the collection of some of these data.

*Present address: Air Products and Chemicals, Inc., Allentown, PA 18195.

†Present address: Department of Chemistry, University of Texas–Austin, Austin, TX 78712-1167.

[1]B. J. Knapp and J. G. Tobin, Phys. Rev. B **37**, 8656 (1988).

[2]G. Le Lay, Surf. Sci. **132**, 169 (1983).

[3]G. Le Lay, G. Quentel, J. P. Faurie, and A. Masson, Thin Solid Films **35**, 273 (1976); **35**, 289 (1976).

[4]M. Bertucci, G. Le Lay, M. Manneville, and R. Kern, Surf. Sci. **85**, 471 (1979).

[5]A. L. Wachs, T. Miller, A. P. Shapiro, and T. C. Chiang, Phys. Rev. B **35**, 5514 (1987).

[6]A. L. Wachs, T. Miller, and T. C. Chiang, Phys. Rev. B **33**, 8870 (1986).

[7]G. Rossi, I. Abbati, L. Braicovich, I. Lindau, and W. E. Spicer, Phys. Rev. B **25**, 3619 (1982).

[8]P. Perfetti, A. D. Katnani, T. X. Zhau, G. Margaritondo, O. Bisi, and C. Calandra, J. Vac. Sci. Technol. **21**, 628 (1982).

[9]P. Perfetti, A. D. Katnani, R. R. Daniels, T. X. Zhau, and G. Margaritondo, Solid State Commun. **41**, 213 (1982).

[10]P. Perfetti, G. Rossi, I. Lindau, and O. Bisi, Surf. Sci. **124**, L19 (1983).

[11]J. E. Demuth, E. J. VonLenen, R. M. Tromp, and R. J. Hamers, J. Vac. Sci. Technol. B **6**, 18 (1988).

[12]E. J. Van Loenen, J. E. Demuth, R. M. Tromp, and R. J. Hamers, Phys. Rev. Lett. **58**, 373 (1987).

[13]R. J. Wilson and S. Chiang, Phys. Rev. Lett. **59**, 2329 (1987).

[14]T. L. Porter, C. S. Chang, and I. S. T. Tsong, Phys. Rev. Lett. **60**, 1739 (1988).

[15]T. Yokotsuka, S. Kono, S. Suzuki, and T. Sagawa, Surf. Sci. **127**, 35 (1983).

[16]F. Houzay, G. M. Guichar, A. Cros, F. Salvan, R. Pinchaux, and J. Derrien, Surf. Sci. **124**, L1 (1983).

[17]G. Le Lay, M. Manneville, and R. Kern, Surf. Sci. **72**, 405 (1978).

[18]G. V. Hansson, R. Z. Bachrach, R. S. Bauer, and P. Chiaradia, Phys. Rev. Lett. **46**, 1033 (1981).

[19]S. Kono, K. Higashiyama, T. Kinoshita, T. Miyahara, H. Kato, H. Ohsawa, Y. Enta, F. Maeda, and Y. Yaegashi, Phys. Rev. Lett. **58**, 1555 (1987).

[20]Aremco Products, Inc., Ossining, NY.

[21]G. Petzow, *Metallographic Etching* (American Society for Metals, Metals Park, OH, 1978), p. 68, chemical etch no. 1.

[22]R. D. Brigans and H. Hochst, Phys. Rev. B **25**, 1081 (1982).

[23]The Ge AES feature (47 eV) generally displayed corresponding behavior (decrease followed by a leveling of intensity). Due to a large background and the relative weakness of this feature, the data were inferior to the metal AES signal.

[24]A Ag(111) ML is equal to 1.9 Ge(111) ML (Ref. 4). The break-in-slope coverage corresponds to 0.87 Ge(111) ML (Ref. 4). The most easily envisioned $\sqrt{3}\times\sqrt{3}$ surface structures should have coverages which are $n(\frac{1}{3})$ Ge(111) ML. The significance of a coverage which is not $\frac{1}{3}$, $\frac{2}{3}$, or 1 is discussed in Ref. 4. A similar situation exists for the case of Ag/Si(111) (Refs. 2 and 11).

[25]J. G. Tobin, S. W. Robey, and D. A. Shirley, Phys. Rev. B **33**, 2270 (1986); J. G. Tobin, S. W. Robey, L. E. Klebanoff, and D. A. Shirley, *ibid.* **35**, 9056 (1987); J. C. Hansen, J. A. Benson, W. D. Clendening, M. T. McEllistrem, and J. G. Tobin, *ibid.* **36**, 6186 (1987).

[26]S. D. Kevan and D. A. Shirley, Phys. Rev. B **22**, 542 (1980); J. J. Barton, C. C. Bahr, S. W. Robey, Z. Hussain, E. Umbach, and D. A. Shirley, *ibid.* **34**, 3807 (1986).

[27]R. Hanson (private communication).

[28]B. J. Knapp, Ph.D. thesis, University of Wisconsin–Madison, 1988.

[29]J. J. Yeh and I. Lindau, At. Data Nucl. Data Tables **32**, 1 (1985).

[30]J. G. Nelson, S. Kim, W. J. Gignac, R. S. Williams, J. G. Tobin, S. W. Robey, and D. A. Shirley, Phys. Rev. B **32**, 3465 (1985).

[31]S. D. Kevan and R. H. Gaylord, Phys. Rev. B **36**, 5809 (1987).

[32]P. S. Wehner, R. S. Williams, S. D. Kevan, D. Denley, and D. A. Shirley, Phys. Rev. B **19**, 6164 (1979).

[33]A. L. Wachs, T. Miller, T. C. Hsieh, A. P. Shapiro, and T. C. Chiang, Phys. Rev. B **32**, 2326 (1985).

[34]G. Apai, S. T. Lee, and M. G. Mason, Solid State Commun. **37**, 213 (1981).
[35]G. Le Lay, M. Manneville, and J. J. Metois, Surf. Sci. **123**, 117 (1982).
[36]B. J. Knapp, J. C. Hansen, J. A. Benson, and J. G. Tobin, Surf. Sci. **188**, L675 (1987).
[37]K. A. Mills, R. F. Davis, S. D. Kevan, G. Thornton, and D. A. Shirley, Phys. Rev. B **22**, 581 (1980).